

# Experimental Analysis of a 4-Qubit Cluster State

Nikolai Kiesel<sup>1,2</sup>, Christian Schmid<sup>1,2</sup>, Ulrich Weber<sup>1,2</sup>, Otfried Gühne<sup>3</sup>, Géza Tóth<sup>2</sup>, Rupert Ursin<sup>4</sup>, Harald Weinfurter<sup>1,2</sup>

<sup>1</sup>Max-Planck-Institut für Quantenoptik, D-85748 Garching, Germany

<sup>2</sup>Department für Physik, Ludwig-Maximilians-Universität, D-80797 München, Germany

<sup>3</sup>Institut für Quantenoptik und Quanteninformation,

Österreichische Akademie der Wissenschaften, A-6020 Innsbruck, Austria

<sup>4</sup>Institut für Experimentalphysik, Universität Wien, A-1090 Wien, Austria

(Dated: October 10, 2018)

Linear optics quantum logic operations enabled the observation of a four-photon cluster state. We prove genuine four-partite entanglement and study its persistency, demonstrating remarkable differences to the usual GHZ state. Efficient analysis tools are introduced in the experiment, which will be of great importance in further studies on multi-particle entangled states.

PACS numbers: 03.67.Mn, 03.65.Ud, 03.67.Hk

Multipartite entangled states play a fundamental role in the field of quantum information theory and its applications. Recently, special types of entangled multi-qubit states, the so-called graph states, have moved into the center of interest [1]. Due to the fact that they can be generated by next-neighbor interactions, these states occur naturally in solid state systems or can be easily obtained in experiments on atomic lattices [2]. These graph states are basic elements of various quantum error correcting codes [3] and multi-party quantum communication protocols [4]. Well known members of this family of states are the GHZ and cluster states. The latter received a lot of attention in the context of the so-called one-way quantum computer scheme suggested by Briegel and Raussendorf [5]. There, the cluster state serves as the initial resource of a universal computation scheme based on single-qubit operations only. Very recently the principal feasibility of this approach was experimentally demonstrated for a four-photon cluster state [6].

In this letter we report the experimental detection of a high fidelity four-photon cluster state. The inherent stability of the linear optics phase gate implemented here allowed a detailed characterization of the states entanglement properties as well as of its entanglement persistency under loss of qubits. Introducing stabilizer formalism [7] for the experimental analysis we were able to detect genuine four partite entanglement and to determine the states fidelity with a minimum number of measurements.

The four-qubit cluster state can be written in the form

$$|\mathcal{C}_4\rangle = \frac{1}{2}(|HHHH\rangle_{abcd} + |HHVV\rangle_{abcd} + |VVHH\rangle_{abcd} - |VVVV\rangle_{abcd}), \quad (1)$$

where  $|H_i\rangle$  and  $|V_i\rangle$  denote linear horizontal (H) and vertical (V) polarization of a photon in the spatial mode  $i$  ( $i = a, b, c, d$ ). If one compares this state with the product of two Bell states  $|\Phi^+\rangle_{ij} = \frac{1}{\sqrt{2}}(|HH\rangle_{ij} + |VV\rangle_{ij})$ , one observes that the states are equal up to a phase factor of the last term. This phase can be generated by a controlled phase (C-Phase) gate acting on input modes

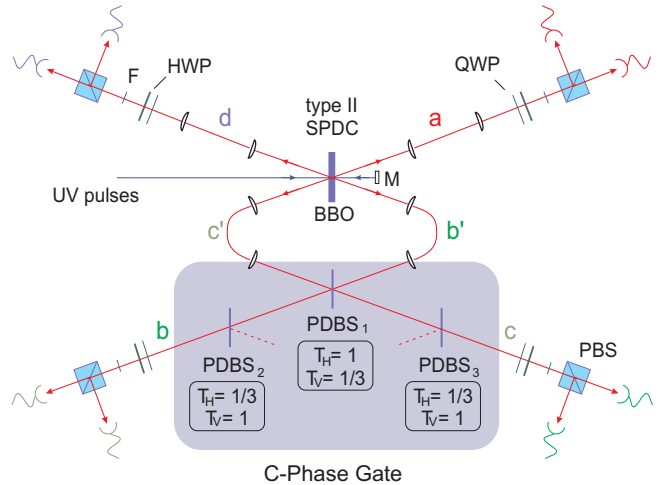


FIG. 1: Experimental setup for the demonstration of the four-photon polarization-entangled cluster state. The state is observed after entangling two EPR-pairs via a linear optics controlled phase gate (C-Phase gate), which employs two-photon interference at polarization dependent beam splitters (PDBS). Two entangled photon pairs are originating from type II spontaneous parametric down conversion (SPDC) by pumping a  $\beta$ -Barium Borate (BBO) crystal in a double pass configuration. Half- and quarter wave plates (HWP, QWP) together with polarizing beam splitters (PBS) are used for the polarization analysis.

$b'$  and  $c'$  as defined by

$$\text{C-Phase gate : } \begin{cases} |HH\rangle_{b'c'} \rightarrow |HH\rangle_{bc} \\ |HV\rangle_{b'c'} \rightarrow |HV\rangle_{bc} \\ |VH\rangle_{b'c'} \rightarrow |VH\rangle_{bc} \\ |VV\rangle_{b'c'} \rightarrow -|VV\rangle_{bc} \end{cases} \quad (2)$$

This scheme directly reflects the generation principle of graph states: evidently, the state  $|\Phi^+\rangle$  can be generated by next-neighbor interaction, and the four-qubit cluster state is then obtained by a third interaction between the neighboring qubits  $b'$  and  $c'$ .

To experimentally implement the C-Phase gate for photons we simplified the linear-optics gate introduced recently [8], thereby enabling its application in a four-photon experiment. Since stability is indispensable in multi-photon experiments we replace (phase-dependent) single-photon interferometers for different polarizations by a polarization dependent (but phase-independent) two-photon interference [9]. It is well known, that in two-photon interference both photons leave the same output of the beam splitter [10]. However, if reflectivity and transmittance are not equal, first, there is a certain probability for the photons to be detected in different outputs, and second, this term of the wavefunction might acquire also a phase shift of  $\pi$ . Using a beam splitter with polarization-dependent splitting ratio (PDBS), one can tune parameters such, that the desired action is achieved for photons leaving the beam splitter in different output ports. Optimal action is achieved, if the gate-input photons are overlapped on a PDBS<sub>1</sub>, with transmission for horizontal polarization  $T_H = 1$ , and for vertical polarization  $T_V = 1/3$ . In order to equalize the transmittance for all input polarizations, beam splitters (PDBS<sub>2</sub> and PDBS<sub>3</sub>) with the complementary transmissions ( $T_H = 1/3$ ,  $T_V = 1$ ) are placed in each output of the overlap beam splitter (see Fig. 1) [9]. All together, the detection probability of coincidences in the output of the gate, and thus the rate of operation, is  $1/9$  independent of the input state.

In the experiment, we use spontaneous parametric down conversion for the preparation of the two EPR pairs. UV pulses with a central wavelength of 390 nm and an average power of 700 mW from a frequency-doubled mode-locked Ti:sapphire laser (pulse length 130 fs) are used in a double pass configuration to pump a 2 mm thick BBO ( $\beta$ -Barium Borate, type-II) crystal to obtain two polarization entangled photon-pairs in distinguishable outputs. Effects originating from double pair emission into one or the other pair of outputs are suppressed as all detections are conditioned to registering one photon in each of the four output modes  $a$ ,  $b$ ,  $c$ , and  $d$ . Coupling the four photons into single mode fibers already behind the BBO-crystal optimizes collection efficiency and exactly defines the spatial modes, the spectral selection is achieved with narrow bandwidth interference filters  $F$  ( $\Delta\lambda = 2$  nm in the C-Phase Gate and  $\Delta\lambda = 3$  nm in modes  $a$  and  $d$ ) before detection. For the initial alignment of the C-Phase gate, first, photons originating from one SPDC process and, second, triggered Hong-Ou-Mandel interference between the photons emerging from the two SPDC-processes is used to set the temporal overlap (see Fig. 1). This setup is sensitive only to length changes on the order of the coherence length of the detected photons ( $\approx 150\mu\text{m}$ ) and thus stays stable over several days with a typical four-fold coincidence count rate of 150 per hour.

Polarization analysis is performed in all of the four outputs. All eight Si-APD single photon counters are fed into a multi-channel coincidence unit which allows to si-

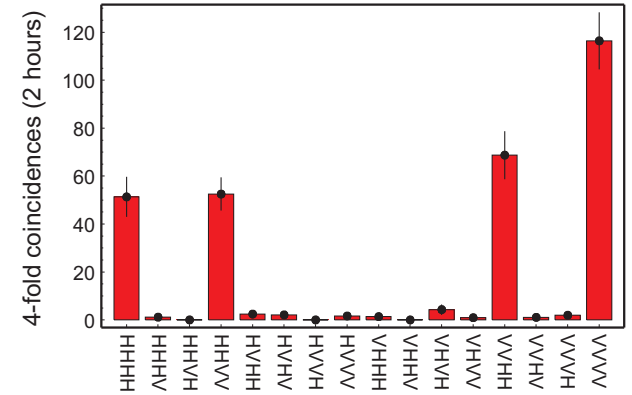


FIG. 2: Four-fold coincidence counts obtained during two hours of measurement when analysing in the H/V - basis in all four output modes.

multaneously register any possible coincidence detection between the inputs. The rates for each of the 16 characteristic four-fold coincidences have to be corrected for the difference in the efficiencies of the detectors. The errors on all quantities are deduced from propagated Poissonian counting statistics of the raw detection events and independently determined efficiencies.

Figure 2. displays the counts obtained for the four-photon cluster state (1). One clearly observes the four-term structure with peaks at  $HHHH$ ,  $HHVV$ ,  $VVHH$ , and  $VVVV$ . The  $VVVV$ -contribution is enhanced, due to non-perfect indistinguishability of the photons at the overlap beam splitter in the phase gate, resulting in additional, polarized noise. These data alone, however, do not prove the contributions to be in a coherent superposition; various bases have to be analyzed. Exemplarily we show the four-photon coincidence counts when the photons in mode  $a$ ,  $b$  (Fig. 3a), or the photons in mode  $c$ ,  $d$  (Fig. 3b), respectively, are measured along  $\pm 45^\circ$ . The clear four term structure is present here as well and indicates the coherence of the cluster state observed. The imperfect interference results in an increase of detections with  $VVxx$  (a), or  $xxVV$  (b), respectively ( $x = +45^\circ/-45^\circ$ ).

Graph states share the common property that an entanglement witness testing four-partite entanglement [11] can be constructed via the so-called stabilizer operators (for the four-qubit case, see Table I), resulting, for the state  $|\mathcal{C}_4\rangle$  in

$$\begin{aligned} \mathcal{W}_{\mathcal{C}_4} := & 3 \cdot \mathbb{1}^{\otimes 4} - \frac{1}{2} \left( \sigma_z^{(a)} \sigma_z^{(b)} + \mathbb{1} \right) \left( \sigma_z^{(b)} \sigma_x^{(c)} \sigma_x^{(d)} + \mathbb{1} \right) \\ & - \frac{1}{2} \left( \sigma_x^{(a)} \sigma_x^{(b)} \sigma_z^{(c)} + \mathbb{1} \right) \left( \sigma_z^{(c)} \sigma_z^{(d)} + \mathbb{1} \right), \quad (3) \end{aligned}$$

with the theoretically optimal value of  $\text{Tr}(\mathcal{W}_{\mathcal{C}_4} \rho_{th}) = -1$  [12]. Thus, the correlations in the two basis settings of Fig. 3 suffice to evaluate the entanglement witness. Experimentally we find  $\text{Tr}(\mathcal{W}_{\mathcal{C}_4} \rho_{exp}) = -0.299 \pm 0.050$  clearly proving the genuine four-photon entanglement of the observed state.

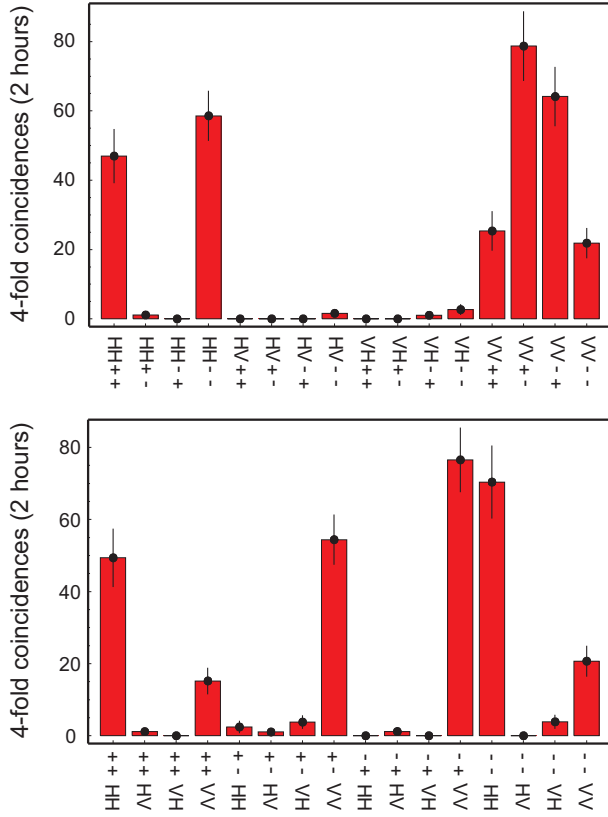


FIG. 3: Four-fold coincidence counts obtained during two hours of measurement when analyzing in the H/V-basis in modes  $a$  and  $b$  and in the  $\pm 45^\circ$ -basis in modes  $c$  and  $d$  (a), or when analyzing in the  $\pm 45^\circ$ -basis in modes  $a$  and  $b$  and in the H/V-basis in modes  $c$  and  $d$  (b), respectively. These data are already sufficient to prove four-photon entanglement based on stabilizer witnesses.

In order to evaluate the quality of the state observed the fidelity  $F_{C_4} = \langle C_4 | \rho_{exp} | C_4 \rangle$  is the tool of choice. In general, full knowledge of the experimental state, and therefore a complete state tomography would be necessary to calculate the fidelity between two states. However, again one can profit from the fact that the cluster state, as a graph state, is completely describable by its stabilizers. Therefore, the fidelity for the cluster state (as for any graph states) equals the average expectation value of the stabilizer operators. A measurement of the respective correlations is thus sufficient to evaluate the state fidelity (Table I). In our case, these are 16 correlations, instead of 81 for full tomography, resulting in a value of  $F_{C_4} = 0.741 \pm 0.013$ .

The stabilizer correlations can be used as well for the construction of a Bell inequality [13] with the following Bell operator:

$$\mathcal{S} = \sigma_z \mathbb{1} \sigma_x \sigma_x + \sigma_x \sigma_y \sigma_y \sigma_x + \sigma_x \sigma_y \sigma_x \sigma_y - \sigma_z \mathbb{1} \sigma_y \sigma_y. \quad (4)$$

The maximal expectation value of  $\mathcal{S}$  is obtained for the cluster state giving the value  $S = \text{Tr}(\mathcal{S}\rho_C) = 4$ , while the bound for local hidden variable models is  $S = 2$ . In

TABLE I: Stabilizer Correlations

|                             | operators   | expectation value |
|-----------------------------|---|-------------------|
| (1)                         | $\sigma_z \otimes \sigma_z \otimes \mathbb{1} \otimes \mathbb{1}$     | $0.935 \pm 0.037$ |
| (2)                         | $\sigma_x \otimes \sigma_x \otimes \sigma_z \otimes \mathbb{1}$       | $0.713 \pm 0.044$ |
| (3)                         | $\mathbb{1} \otimes \sigma_z \otimes \sigma_x \otimes \sigma_x$       | $0.638 \pm 0.045$ |
| (4)                         | $\mathbb{1} \otimes \mathbb{1} \otimes \sigma_z \otimes \sigma_z$     | $0.931 \pm 0.036$ |
| (5)                         | $-\sigma_y \otimes \sigma_y \otimes \sigma_z \otimes \mathbb{1}$      | $0.679 \pm 0.043$ |
| (6)                         | $\sigma_z \otimes \mathbb{1} \otimes \sigma_x \otimes \sigma_x$       | $0.707 \pm 0.045$ |
| (7)                         | $\sigma_z \otimes \sigma_z \otimes \sigma_z \otimes \sigma_z$         | $0.931 \pm 0.064$ |
| (8)                         | $\sigma_x \otimes \sigma_y \otimes \sigma_y \otimes \sigma_x$         | $0.729 \pm 0.062$ |
| (9)                         | $\sigma_x \otimes \sigma_x \otimes \mathbb{1} \otimes \sigma_z$       | $0.673 \pm 0.044$ |
| (10)                        | $-\mathbb{1} \otimes \sigma_z \otimes \sigma_y \otimes \sigma_y$      | $0.626 \pm 0.067$ |
| (11)                        | $\sigma_y \otimes \sigma_x \otimes \sigma_y \otimes \sigma_x$         | $0.628 \pm 0.066$ |
| (12)                        | $-\sigma_y \otimes \sigma_y \otimes \mathbb{1} \otimes \sigma_z$      | $0.690 \pm 0.060$ |
| (13)                        | $-\sigma_z \otimes \mathbb{1} \otimes \sigma_y \otimes \sigma_y$      | $0.616 \pm 0.067$ |
| (14)                        | $\sigma_x \otimes \sigma_y \otimes \sigma_x \otimes \sigma_y$         | $0.681 \pm 0.066$ |
| (15)                        | $\sigma_y \otimes \sigma_x \otimes \sigma_x \otimes \sigma_y$         | $0.681 \pm 0.064$ |
| (16)                        | $\mathbb{1} \otimes \mathbb{1} \otimes \mathbb{1} \otimes \mathbb{1}$ | $1.00 \pm 0.017$  |
| $F_{exp} = 0.741 \pm 0.013$ |   |                   |

our experiment we reach  $S = \text{Tr}(\mathcal{S}\rho_{exp}) = 2.73 \pm 0.12$  clearly violating the classical bound.

Note, this Bell inequality is *not* violated by GHZ states, which is a further indication of the cluster state showing a different kind of entanglement compared to the GHZ state. Further differences arise for the persistency of the entanglement, that is the entanglement under projection or loss of particles [14].

A projective measurement onto  $\sigma_x$ , which corresponds to a projection onto the states  $|\pm 45^\circ\rangle$  reduces both the four-photon GHZ state and the cluster state to a three photon GHZ state. Still, the resulting entanglement persistency is remarkably different. Depending on the result of the projection measurement (i.e. "+45°" or "-45°"), the four-photon GHZ state reduces to  $|GHZ\rangle_3^\pm = (|HHH\rangle \pm |VVV\rangle)/\sqrt{2}$ , the incoherent sum of these two states exhibits no entanglement or coherence whatsoever. Contrary, for the four-photon cluster state we obtain, depending on the measurement result in mode  $d$

$$\begin{aligned} |\mathcal{C}_3\rangle_{abc}^\pm &= (|HH\pm\rangle_{abc} + |VV\mp\rangle_{abc})/\sqrt{2} \\ &= (|\Phi^+\rangle_{ab}|H\rangle_c \pm |\Phi^-\rangle_{ab}|V\rangle_c)/\sqrt{2}. \end{aligned} \quad (5)$$

According to the rules [14], this is again a cluster state, which can be further reduced, e.g. by projecting the photon in mode  $c$  onto  $|H\rangle/|V\rangle$ , to the two-photon cluster states  $|\Phi^\pm\rangle$ . The incoherent sum of the states of Eq. (5) gives the state  $\rho_{a,b,c}$  which results from the loss of photon  $d$ . This state still exhibits two-partite entanglement. To test these properties we apply the entanglement witnesses for the respective states, which again follow from

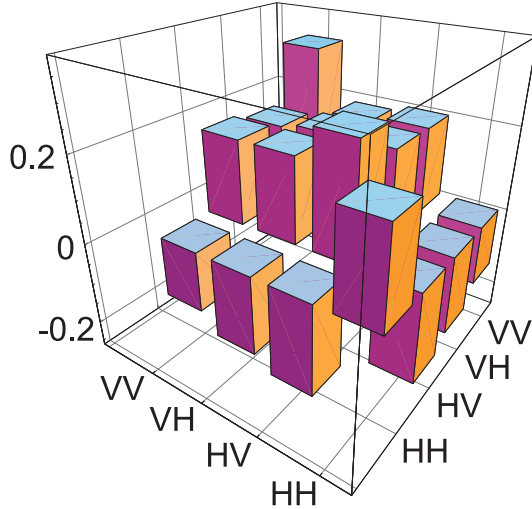


FIG. 4: State tomography after projection of photons in mode  $b$  and  $c$  onto  $-45^\circ$ . The state  $(|H-\rangle_{ad} - |V+\rangle_{ad})/\sqrt{2}$  is indeed obtained with a fidelity of  $0.809 \pm 0.027$ .

the stabilizer formalism [12] as

$$\mathcal{W}_{C_{3,abc}^\pm} = \frac{3}{2} \cdot \mathbb{1}^{\otimes 3} - \sigma_x^{(a)} \sigma_x^{(b)} \sigma_z^{(c)} - \frac{1}{2} \left( \sigma_z^{(a)} \sigma_z^{(b)} \mathbb{1}^{(c)} \pm \sigma_z^{(a)} \mathbb{1}^{(b)} \sigma_x^{(c)} \pm \mathbb{1}^{(a)} \sigma_z^{(b)} \sigma_x^{(c)} \right); \quad (6)$$

$$\mathcal{W}_{(\rho_{abc})} = \mathbb{1}^{\otimes 3} - \sigma_z^{(a)} \sigma_z^{(b)} \mathbb{1}^{(c)} - \sigma_x^{(a)} \sigma_x^{(b)} \sigma_z^{(c)}. \quad (7)$$

In the experiment we observed the states with a fidelity of  $F_{C_{3,abc}^+} = 0.756 \pm 0.028$  and  $F_{C_{3,abc}^-} = 0.753 \pm 0.026$ , yielding expectation values of the entanglement witnesses of  $\langle \mathcal{W}_{C_{3,abc}^+} \rangle = -0.362 \pm 0.090$ ,  $\langle \mathcal{W}_{C_{3,abc}^-} \rangle = -0.392 \pm 0.082$ , and  $\langle \mathcal{W}_{(\rho_{abc})} \rangle = -0.648 \pm 0.057$ , respectively. We obtain similar results for the witnesses when projecting and tracing over other photons, indicating the high degree of entanglement persistency of the cluster state.

Finally, if we project two of the four photons onto suited bases, we obtain two-photon entanglement for the remaining ones, which reflects the maximum connectivity of the cluster state [14]. In the scheme of the one-way quantum computer, such a two-photon measurement corresponds to defining the input values for a CNOT operation [6]. For example, if one projects/initializes photons in modes  $b$  and  $c$  to, say both  $| -45^\circ \rangle$ , photons in modes  $a$  and  $d$  are due to the CNOT plus Hadamard operation in the state  $(|H-\rangle_{ad} - |V+\rangle_{ad})/\sqrt{2}$ . Fig. 4 shows the full state tomography for this case. We experimentally obtain a fidelity relative to the above state of  $0.809 \pm 0.027$ , resulting in a logarithmic negativity [15] for the observed entanglement of  $0.718 \pm 0.047$ .

In summary we have presented a scheme for the preparation of a four-qubit entangled cluster state in the polarization degree of freedom of photons. This scheme is the first application of a new and simple way for the experimental realization of a C-Phase gate based on linear optics. The high stability and quality of the state creation enabled a detailed experimental characterization of the entanglement properties of a four-photon cluster state, including demonstration of its genuine four-qubit entanglement and the study of entanglement persistency under selective measurements and loss of one or two qubits. We applied entanglement witnesses and introduced a simplified fidelity analysis, which allows definite characterization even without full state tomography. Such analysis will become even more crucial in experiments with higher numbers of qubits, where the effort for full state tomography increases exponentially. The detailed study forms the basis to evaluate the applicability of the experimental state for further quantum information tasks, for example for multi-partite quantum cryptography and one-way quantum computation.

This work was supported by the Deutsche Forschungsgemeinschaft and the European Commission through the EU Project RamboQ (IST-2001-38864).

---

[1] W. Dür, H. Aschauer, H.J. Briegel, Phys. Rev. Lett. **91**, 107903 (2003); M. Hein, J. Eisert, H.J. Briegel, Phys. Rev. A **69**, 062311 (2004).

[2] O. Mandel, M. Greiner, A. Widera, T. Rom, T.W. Hänsch, I. Bloch, Nature **425**, 937 (2003).

[3] D. Schlingemann and R.F. Werner, Phys. Rev. A **65**, 012308 (2002).

[4] R. Cleve and H. Buhrman, Phys. Rev. A **56**, 1201 (1997); M. Zukowski et al., Acta Phys. Pol. **93**, 187 (1998); M. Hillery, V. Buzek, and A. Berthiaume, Phys. Rev. A **59**, 1829 (1999); R. Cleve, D. Gottesmann, and H.-K. Lo, Phys. Rev. Lett. **83**, 648 (1999).

[5] R. Raussendorf and H.J. Briegel, Phys. Rev. Lett. **86**, 5188 (2001); M.A. Nielsen, Phys. Rev. Lett **93**, 4 (2004).

[6] P. Walther et al., Nature **434**, 169 (2005).

[7] G. Tóth, O. Gühne, e-print quant-ph/0501020.

[8] T.C. Ralph, N.K. Langford, T.B. Bell, and A.G. White, Phys. Rev. A **65**, 062324 (2002); H.F. Hofmann, S. Takeuchi, Phys. Rev. A **66**, 024308 (2002); J.L. O'Brien, G.J. Pryde, A.G. White, T.C. Ralph and D. Branning, Nature **426**, 264 (2003); J.L. O'Brien et al., Phys. Rev. Lett. **65**, 062324 (2002).

[9] N. Kiesel, to be submitted.

[10] C.K. Hong, Z.Y. Ou, L. Mandel, Phys. Rev. Lett. **59**, 2044 (1987).

[11] M. Bourennane et. al. , Phys. Rev. Lett **92**, 087902 (2004).

[12] G. Tóth and O. Gühne, Phys. Rev. Lett **94**, 060501 (2005).

[13] V. Scarani, A. Acín, E. Schenck, M. Aspelmeyer, Phys. Rev. A **71**, 042325 (2005).

[14] H.J. Briegel and R. Raussendorf, Phys. Rev. Lett **86**, 910 (2001); M. Eibl et. al., to appear in Phys. Rev. Lett..

[15] K. Zyczkowski, P. Horodecki, A. Sanpera, and M. Lewenstein, Phys. Rev. A **65**, 062324 (2002); H.F. Hofmann, S. Takeuchi, Phys. Rev. A **66**, 024308 (2002); J.L. O'Brien, G.J. Pryde, A.G. White, T.C. Ralph and D. Branning, Nature **426**, 264 (2003); J.L. O'Brien et al., Phys. Rev. Lett. **65**, 062324 (2002).

stein, Phys.Rev. A **58** 883 (1998).